Partial coated stem cells with bioinspired silica as new generation of cellular hybrid materials

Marta M. Maciel, Tiago R. Correia, Vítor M. Gaspar, João M. M. Rodrigues, Insung S. Choi, João F. Mano**

Marta M. Maciel, Dr. Tiago R. Correia, Dr. Vítor M. Gaspar, Dr. João M. M. Rodrigues, Prof. João F. Mano
CICECO, Aveiro Institute of Materials
Department of Chemistry, University of Aveiro
Complexo de Laboratórios Tecnológicos, Campus Universitário de Santiago, 3810-193 Aveiro, Portugal
E-mail: trcorreia@ua.pt; jmano@ua.pt;

Marta M. Maciel
CEB, Centre of Biological Engineering
University of Minho
Campus de Gualtar, 4710-057, Braga, Portugal

Prof. Insung S. Choi
Center for Cell-Encapsulation Research, Department of Chemistry
KAIST, Daejeon 34141, Korea

Keywords: advanced cell-material interactions, cell-based materials, organic-inorganic hybrid composites, cell partial coatings, sol-gel processes

Abstract

The manipulation of cell surface in anchorage-dependent cells can help overcome difficulties presented during cell handling and application. Silica-based protective mechanisms existing in free-floating microorganisms may be used as inspiration for sustaining human cells survival in suspension. Gathering on this, herein human adipose-derived mesenchymal stem cells (hASCs) were partially coated with a hard silica layer that operates as a supporting platform for individual cells in suspension. Inspired by the organic templates involved in biosilicification, a novel chitosan (CHT) derivative displaying fully natural quaternary amine moieties was synthetized via a rapid, one-pot strategy. Silicification was promoted on individual hASCs surface via a two steps process: a priming step onto previously adhered cell with this CHT derivative, followed by a biocompatible sol-gel process. hASCs holding a silica backpack exhibited enhanced cell survival in suspension conditions and could spread and acquire a more

adherent phenotype. This new protocol for cell surface modification also provides a new generation of hybrid materials with functionalization of the silica backpack which can be applied to different areas from tissue engineering, biosensing, drug delivery and targeted cell-based therapies.

1. Introduction

Innumerable developments have been accomplished, in cell therapy and tissue engineering, to promote the repair and regeneration of damaged tissues during the last 20 years. Even though there has been an increased knowledge and knowhow in this field, the practical implementation still shows lots of failures with only a few scattered solutions being applied to patients. This could be caused by a multitude of factors, such as low cell survival, lack of similar structures to native tissue, and the absence of cellular functionality.[1] Different concepts have also been exploited towards replicating in vitro the complexity and functionality presented by some tissues of the human body, such as bone or skin. For example, bottom-up regenerative-medicine approaches offer the possibility for generating highly organized tissues by passive or directed assembly of living building blocks including cell sheets or 3D spheroids.[1-2] However, these building blocks are highly complex both structurally and functionally, and raise challenges concerning fabrication time, and limitations in cell types and densities. In this respect, employing simpler building blocks such as engineered single cells could allow for new possibilities, from a higher control over cell arrangement, to the assembly of more complex 3D constructs that recapitulate tissues cellular heterogeneity. Moreover, cell-surface modification strategies would enable the control of cellular behavior and fate at the single-cell level.

Cell modification has been engineered by various strategies, such as cell surface functionalization, coating, and encapsulation, to accomplish different goals, including cytoprotection, improvement of mechanical resistance, drug delivery, and targeting.

Particularly, single cell nanoencapsulation enables the fabrication and manipulation of single cells, protecting and improving their viability without affecting the cell's genetic code.[3] Various chemical strategies have been developed, from single-step or sequential electrostatic-mediated multilayer deposition of polyelectrolytes and formation of metal-organic species to biomineralization.[4] Biomineralization is a natural process, by which living organisms produce minerals from bioorganic molecules and inorganic solids, exemplified by bone and teeth formation in human. In particular, the formation of biogenic silica (biosilicification) or calcium carbonate (biocalcification) provides the support and protection against environmental stresses and predators.[5] Among the different classes of biominerals, silica is a remarkable biomaterial that possesses a wide range of characteristics like mechanical strength, chemical inertness, hydrophilic character, and has a relevant role in bone and connective tissue formation.[6] It can be easily produced under mild conditions, giving the opportunity to obtain new materials with both advanced structural and multifunctional properties; silica-based materials can be conjugated with highly sensitive compounds like biomolecules and enzymes and give rise to bioactive compounds.[7] In nature, diatoms are a major group of unicellular eukaryotic algae present in marine and freshwater ecosystems and are known to produce silica walls in a variety of forms and shapes.[8] Inspired by the biosilicification, individual yeast and mammalian cells have been fully encapsulated with silica-based materials.[9] For example, Jurkat cells were fully encapsulated with polyethyleneimine (PEI) as a primer for inducing and regulating the silica shell formation from tetramethyl orthosilicate (TMOS) and (3-mercaptopropyl) trimethoxysilane.[9b] The resulting silica-encapsulated cells displayed an enhanced survival rate against enzymatic attack, that decreases in long-term, due to the complete entrapment within silica shells. It remains challenging how cell protection could be achieved while maintaining cell viability and functions in adverse conditions.

We envisaged that the partial encapsulation of anchorage-dependent cells with silica, forming a silica backpack, would lead to self-supporting cells, in which the hard-partial coating could not only make the cells survive longer in unfavorable suspension environments, but also enable the control of single-cell fate without compromising cell's normal behavior. In this study, we report an advanced approach for cell-surface functionalization by partially coating individual human adipose stem cells (hASCs) with a silica layer, offering a novel concept of creating tough supports for attachment-dependent cells incubated in suspension conditions. On a simple, environmentally friendly, and customizable functionalization strategy we developed a new chitosan (CHT) derivative that enabled silica deposition to the cell membrane without significant loss in cell viability and fully characterized the resulting hybrid systems. In addition to the maintained cell viability and function, we hypothesize that the silica backpack could provide the support for other cells, permitting the creation of large cellular aggregates and accelerating new microtissues formation.

2. Results and Discussion

2.1. Development of silica partial coated cells

The formation of partial silica coating (silica backpack) on individual hASCs was achieved by two simple steps, namely bioinspired priming and silicification, represented in **Figure 1** A-D. Although biosilicification occurs under physiological conditions in certain organisms, the fragility of mammalian cell membranes does not allow this process to be applied directly to mammalian cells. Thus, cell surface modifications must be performed under well designed conditions in a short time-window, to not compromise cell integrity and viability. For example, the direct use of a silica solution, usually prepared under acid or basic conditions, is too aggressive for the cell membrane that protects the cell from external aggressions as a thin barrier, but can be easily disrupted in harsh environments.[6a] Additionally, it would require much time

for silica to interact with the cell membrane due to their negative charges.[10] Modification of the cells surface can be achieved through different methods including genetic strategies or non-genetic modification approaches such as: i) covalent conjugation to the amino groups of biomolecules on the surface of cells, ii) incorporation of amphiphilic polymers into the lipid bilayer via hydrophobic interactions or iii) adsorption of charged macromolecules through electrostatic interactions.[4a, 11] Among them, approaches involving electrostatic interactions present interesting advantages. For example, it enables the use of layer-by-layer processes for the deposition of other compounds. In addition, the functionalization chemistry involved is simple and inexpensive, and is not specific for a unique cell type. [10, 12]

On the other hand, the chemical composition of silica cell wall in diatoms includes organic molecules besides the presence of silica, and the 3 major organic groups are phosphoproteins (silaffins), long-chain polyamines (LPAs), and acid proteins (silicidins). These biomolecules are the key factors in the biosilicification process due to their roles in inducing and regulating the rapid precipitation of silica under physiological conditions.[13] In the bioinspired silicification for single-cell nanoencapsulation, PEI, a highly positively charged polycation, has been used for mimicking the LPAs, as it is highly branched for rapid silica formation, but the cell viability was lowered due to its highly positively charged character.[9b, 11, 14] The use of polycations with high positive charge is generally known to be lethal to cells, especially mammalian cells in cell-surface engineering approaches.[10, 14]

CHT is a naturally available linear amino-polyssaccharide, which is biocompatible, biodegradable and versatile in chemical modifications. It has previously been used for the production of CHT-silane thin films.[15] However, CHT exhibits poor solubility at physiological pH, due to the hydrogen bonds established between the primary amino groups and free hydroxyl groups of the polymer chains, and, therefore, cannot be applied directly for cell-surface engineering. We synthesized a novel CHT derivative by grafting a naturally occurring amino

acid displaying functional quaternary amines, an approach that was inspired by the LPAs found in diatoms.[8b] Particularly, through a rapid, completely organic solvent-free, one pot approach, we introduced the quaternary amines to the CHT polymeric backbone by using a natural compound, L-carnitine (CAR, pKa ~3.8), found in most mammalians (e.g. cardiac and skeletal muscle), plants, and some bacteria.[16] The CHT-carnitine (CHT-CAR) was soluble at physiological pH. The degree of substitution was calculated to be approximately 28 %, based on ^{1}H NMR spectrum analysis (Figure 1 E). The attenuated total reflectance-Fourier transform infrared spectroscopy (ATR-FTIR) spectrum showed a sharp band at 1631 cm^{-1}, corresponding to the C=O stretching, evidencing the presence of CAR in the structure. In addition, the absence of the band at 1584 cm^{-1}, assigned to the NH_2 vibration, indicated that the modification occurred at the amino group, confirming the successful modification (Figure S1-S3).[17]

To achieve only partial silica coating, the cells were attached on an adherent surface prior to the silicification process. With this strategy, only part of the cell surface was available for chemical modification. Briefly, hASCs were seeded at a low density 125 000 cells per petri dish to allow each cell to be single modified using alpha minimal essential medium (α-MEM) supplemented with 10% fetal bovine serum (FBS) and 1% of penicillin and streptomycin (P/S). After washing with α-MEM with 1% P/S (FBS-free α-MEM; pH 7.4), the cells were primed with CHT-CAR (0.4 mg mL^{-1}), previously dissolved in phosphate buffered saline (PBS; pH 7.4), and incubated for 10 min, at 37 °C. The low concentration of CHT-CAR allowed for the maintenance of cell membrane integrity and the formation of a thin and stable CHT-CAR layer through electrostatic and dipole-dipole interactions (Figure 1 B).[18]

Tetraethyl orthosilicate (TEOS) was used as silica source for bioinspired silicification because it is less toxic than TMOS. The silica production via sol-gel process using TEOS has been well described in the literature.[19] (3-Aminopropyl)triethoxysilane (APTES) was additionally used to introduce free amino groups in the silica structure for further chemical functionalization.[20]

After priming with CHT-CAR, the cells were washed with FBS-free α-MEM and incubated for 20 min in a mixture solution of FBS-free α-MEM, TEOS and APTES, washed with FBS-free α-MEM, and incubated in α-MEM for 8 h at 37 °C, followed by detachment and collection of the cells (Figure 1 C).

2.2. Characterization of hASCs partial coated cells

To fully characterize the processes and confirm the formation of silica backpacks, we acquired fluorescence and optical microscopy images at different steps of the coating processes. For fluorescence imaging, we conjugated fluorescein 5(6)-isothiocyanate (FITC) to CHT-CAR (Figure 1 B) and for optical imaging we stained the silica with Alcian blue, a staining agent normally used in histology, displaying a blue colored silica (Figure 1 C).[21] The fluorescence images confirmed that both CHT-CAR and silica were present only on the cell surface.

After detachment of the modified cells, we characterized the silica distribution by laser-scanning confocal microscopy (LSCM), while the cells were in suspension. The 3D reconstruction (z-stack) of images arguably confirmed that the partial silica coating, forming the silica backpack, was achieved for individual hASCs (Figure 1 D). Flow cytometry was performed to assess the percentage of the silica-backpacked cells, after staining the cells with a cell tracking dye (DID) and the silica backpack with FITC (Figure 1 F)**.** The analysis showed that around 57% of the cells are positive for both FITC and DID. Cells with low FITC signal were not considered for the population in the region of interest (Figure S4). We thought that the coating value was reasonably high, considering the constant morphological cellular changes on the culture substrate and the time-wise heterogeneity of cell membranes. The dynamic character of cell membranes also made the silica backpacks differ in their shape and location from cell to cell.[22] Furthermore, this final formulation was achieved after testing different parameters, namely, the amount and nature of silica sources, time deposition of the primer and silica

solutions. From those, the most important was the deposition time where shorter times did not allow cells to acquire a visible silica backpack formed at their surface while longer times induced a significant condensation process of silica between the partial shells of each cell and compromised the formation of cell individual supports.

Nonetheless, these new hybrid cells in the suspension environment could provide a new conceptual development for the field of bottom-up tissue engineering and cell therapy by demonstrating the artificial (partial) support for anchorage-dependent cells in suspension. Specifically, the methodology provides hASCs a surface where they can attach, spread, and proliferate, as the silica backpack would offer anchorage points, mimicking, in a certain way, the adherence stimulus even in a suspension environment. Furthermore, the modified cells containing the silica-based partial supports will also be able to recruit other cells by providing adherent zones in the external part of their self supports, allowing the mobilized cells to spread and elongate, adopting a morphology similar to that shown by the cells in the adherent surfaces.

2.3. Study of silica partial coated cells in a suspension environment

To investigate the effects of silica backpacks on cellular activities such as metabolism, we cultured the cells with silica backpacks (hASC@SiO_2BP) with a low density in flat ultralow adhesion well plates, with wild-type cells as a control, to make the cells dispersed well and not form any types of aggregates in culture media. We observed significant differences in the first 24 h in the suspension environment as single cells of control are almost nonexistent, as they start to aggregate quicker than the cells with silica backpacks which maintained longer their singularity **(Figure 2** A**)**. Moreover, hASC@SiO_2BP showed higher metabolic activity than controls, indicating that their biological functions were not compromised after coating (Figure 2 B and C). We hypothesize that silica backpacks acted as a mechanical support with sufficient

anchorage points and allowed hASC@SiO_2BP to maintain their functions even after detachment from the culture surface. So far, researchers have been inefficient to provide anchorage-dependent cells with tough support maintains cell viability in suspension while enhancing cellular activities, despite many applications, like microfluidics and 3D bioprinting or injection for cell therapies, often use cells in a suspension state. We designed an injection assay to demonstrate that partial coated cells exhibit a higher ability to support shear stress along the flow through a channel. Cells suspensions in a sodium alginate hydrogel (2 % w/v in PBS pH=7.4) circulating with a continuous flow rate (30 mL/h), showed that hASC@SiO_2BP presented a higher survival rate then cells without the partial coating, thus confirming the potential of this technology in applications like 3D bioprinting or injection-based cell therapies (Figure S5).

hASCS, as anchorage-dependent cells, tend to aggregate, while staying in suspension, for survival, and re-establish cell-to-cell contacts. To investigate whether the silica backpacks influenced the aggregation process, we maintained the cells in the suspension conditions for 7 days to ensure that complete aggregates were formed. Both hASC@SiO_2BP and control (uncoated) cells aggregated at day 3, and the aggregates become more defined and shaped at day 7. After 7 days of culture, both hASC@SiO_2BP and the control were viable (Figure 2 A). To further confirm the results, an apoptosis and necrosis assay was also performed, confirming the viability of both hASC@SiO_2BP and control aggregates (Figure S6 B).

Of interest, the cells in the peripheric region of the control aggregates at day 1 are already in an early apoptotic state compared with single hASC@SiO_2BP. Upon day 7, cells in control aggregates are still entering both early and late apoptosis in the peripheric region. We also verified that the size and form of the aggregates differed. The control aggregates (138.2 ± 34.2 μm) were smaller than those of hASC@SiO_2BP (198.3 ± 16.3 μm) (Figure S6 D), showing a more spheroidal shape type than hASC@SiO_2BP which are larger and the aggregate shape is

not defined. We hypothesized that during the aggregate formation of hASC@SiO_2BP, cells could adhere to the silica backpacks of other cells and therefore can spread and elongate more than the controls originating these undefined and larger aggregates. The incorporation of silica and the differences in the surface of the cell aggregates at day 7 were further studied by scanning electron microscopy (SEM) and energy-dispersive X-ray spectroscopy (EDS). The EDS analysis confirmed the presence of silica in the aggregates (Figure 2 D). Furthermore, hASC@SiO_2BP seemed to spread and elongate more at the surface of the aggregates than the controls as we thought, which was additionally supported by the SEM images (Figure S7 A).[23] Additionally, we started to investigate the formation of cell aggregates with these silica backpacks. The results showed that cell aggregates from day 3 stained with N-cadherins (cell-cell contacts) and ZO1 (tight junctions) can stablish cell contacts. Concerning tight junctions, the aggregates formed from the silica partial coatings have less expression presumably because cells are establishing contacts with silica partial coating (Figure S7 B). The samples at days 1 and 7 were fixed, and the cellular components were stained to study the cell's interactions with the silica backpacks (Figure 2 E). The LSCM images showed that the silica backpacks (green) not only were linked to the cell membrane but also enabled other cells to sense the hard silica interface, allowing the cells to acquire a normal spreading shape.

In addition, hASC@SiO_2BP displayed a higher number of focal adhesion points, as well as longer actin filaments than the control: see red arrows in Figure 2 E indicating the more prominent actin filaments. These results can be important when guiding cell differentiation, especially for osteogenic lineage. Polymeric coatings in cells tend to be too soft and avoid cell spreading. Due to that, cells adopt a more spherical morphology with tendency towards adipogenic differentiation.[24] Our results show that cells are sensing silica as a stiff material allowing cells to spread which is important for cells to differentiate towards bone lineage cells.[25]

We also investigated the adherence capacity of the single cells and aggregates by using an adherent surface. The hASC@SiO_2BP aggregates successfully adhered to the provided surface, proving their normal function (Figure S6 C) as well as showing potential for the formation of microscale tissues. Such results strengthen the potential of the proposed methodology as a simple, inexpensive and reproducible strategy for cell surface modification compared to other encapsulation methods [4b, 9b] using organic and inorganic materials and without compromising normal cell functions.

3. Conclusion

Cell surface engineering is one of the most interesting approaches in cell manipulation nowadays. We developed an advanced chemical strategy to partially modify the cell surface in a mild and controlled manner way and generate a new class of cellular hybrid structures armed with silica backpacks. The formation of silica backpacks on individual hASCs was achieved, without compromising cell viability, by using the electrostatic interactions established between the cell membrane and CHT-CAR and, subsequently, with silica formed *in situ*. Without using highly charged polycations, we developed a cytocompatible method quite versatile that could be virtually applied to any other cell types. Another important characteristic of silica is mechanical strength, which in this work was highlighted through the formation of a tough silica backpack on the extracellular membrane that allowed cells to self-support in environmental conditions, and, more significantly, the backpack enhanced cell survival in suspension environments. This is a crucial condition when functional cells are subjected to applications like inject-based, 3D bioprinting, or microfluidics, where the shear stress in cells membranes can lead to their disruption. We also confirmed that the silica-backpacked hASCs acquired a similar phenotype to that of the cells in adherent state, while forming larger aggregates than

pristine cells. Such characteristic suggests the potential of the backpacked hybrid cells in the areas like drug delivery or stem cell differentiation, through the tailored modification of the backpack with different molecules and biochemical cues.

In fact, one of the most interesting features of these new hybrid cells is the potential to be explored in future applications with silica functionalization using other molecules and functional groups. This protocol allows the easy manipulation of silica partial coating with potential to lead the development of new materials formed from these hybrid cells. Moreover, future work is encouraged to understand the silica-cell interactions in the silica-backpacked cells and to explore the application of this developed protocol to other cell types for cell differentiation, sensing, drug delivery, and targeting to specific tissues/organs.

4. Experimental Section

Chitosan (CHT) ChitoClear 43010 TM4779 was kindly provided by Primex EHF with deacetylation degree of 96.6%, molecular weight of 133 760 Da and used without further purification. MES hydrate was purchased from Alfa Aesar, Thermo Fischer Scientific.

L-Carnitine hydrochloride (CAR), 1-(3-Dimethylaminopropyl)-3-ethylcarbodiimide hydrochloride (EDC) and *N*-Hydroxysuccinimide (NHS) were acquired from TCI Chemicals. Tetraethyl orthosilicate (TEOS) reagent grade, 98%, fluorescein 5(6)-isothiocyanate (FITC), Alcian Blue 8GX certified biological stain (AB), hydrochloric acid 37% (HCl), glutaraldehyde, sodium cacodylate, formaldehyde, Triton X-100, low viscosity alginic acid (alginate) sodium salt from brown algae and phosphate buffered saline (PBS) were purchased from Merck. 3-aminopropyltriethoxysilane (APTES) was acquired from Enzymatic S.A. Dulbecco's phosphate buffered saline (DPBS) powder without calcium/magnesium for cell culture was obtained from Corning. Ethanol absolute (EtOH) was obtained from JMGS.

Chitosan-Carnitine (CHT-CAR) synthesis. CHT-CAR was produced by using a one-pot, organic solvent free, EDC/NHS mediated coupling chemistry. CHT (500 mg, corresponding to 2.32 mmol D-amino glucose repeating unit) was dissolved in 100 mL of 0.1 M of MES buffer at pH 5.5 under magnetic stirring. Afterwards CAR (461 mg, 1 equiv, 2.32 mmol), EDC (671 mg, 1.5 equiv, 3.48 mmol) and NHS (402 mg, 1.5 equiv, 3.48 mmol) were separately dissolved in 0.1 M MES buffer and the pH was adjusted to 5.5 to each solution. CAR was mixed with EDC and then added to the CHT solution. After 10 min, NHS was added, and the reaction was kept under magnetic stirring for 24 h, at room temperature (*RT*). Afterwards, the reaction solution was transferred to dialysis bags (MWCO 3.5 kDa) and dialyzed in distilled water (dH_2O) under 7 days, at pH 6.5, adjusted with HCl 5 M solution. After completing the dialysis, the solution was placed in -80 ºC freezer and then freeze dried (LyoQuest Plus Eco). Liquid ^{1}H and ^{13}C NMR spectra were recorded on a Bruker Avance-300 spectrometer operating at 300.13 and 75.47 MHz, respectively, in D_2O solvent. Tetramethylsilane was used as internal reference. ^{1}H NMR was performed with 512 scans at 60 ºC, and the degree of substitution was calculated according to the equation described in the literature.[26] Attenuated total reflectance-Fourier transform infrared spectroscopy (ATR-FTIR) was performed using a Bruker Alpha infrared spectrometer controlled by the OPUS software package (version 7.0). Background and sample measurements were performed in a range between 4000 and 500 cm^{-1} with a resolution of 4 cm^{-1} and averaging 256 scans, at *RT* and with controlled humidity.

Cell culture. Human adipose stem cells (hASCs) were isolated from subcutaneous adipose tissue obtained by liposuction. The human tissues were obtained under a cooperation agreement between Compass Research Group and Hospital da Luz of Aveiro, after approval of the Competent Ethics Committee (CEC) and handled in accordance with the guidelines approved by the CEC. Informed consent was obtained from all subjects. Briefly, samples were transported

in PBS supplemented with 10% of penicillin-streptomycin (P/S) (Thermo Fisher Scientific) and kept at 4 °C. The lipoaspirates were washed thoroughly with PBS and incubated with collagenase type I (0.1% w/v) for 45 min at 37 °C in a shaking water bath. The samples were then centrifuged at 1200 rpm for 10 min and supernatant was removed. Then DPBS was added and then the samples were centrifuged again at 1200 rpm for 5 min. To isolate the hASCs, the pellet was resuspended in minimum essential medium alpha (α-MEM) (Thermo Fischer Scientific) supplemented with 2.2 g L^{-1} sodium bicarbonate (Merck), 10% heat-inactivated fetal bovine serum (FBS) (Thermo Fischer Scientific) and 1% P/S. Culture medium was changed 48 h after initial plating and changed every 3-4 days.

To confirm the successful isolation of hASCs, the phenotypic expression of standard mesenchymal was assessed (98.9% of CD90-AlexaFluor647, 99.6% of CD73-PE 328116, 344004; BioLegend, 87.8% of CD105-FITC, Citomed, 130-098-774), hematopoietic (0.4% of CD34-FITC, BioLegend, 343604) and endothelial (0.1% of CD31-APC, BioLegend, 303116) markers. Previously, cells were harvested using TrypLE™ Express solution (Gibco) at 37 °C for 5 min, and centrifuged. hASCs were resuspended in PBS solution containing 2% (w/v) FBS and the specified antibodies diluted as manufacturer instructions. After 1 h at *RT*, samples were washed with PBS, centrifuged, fixed in PBS with 1% (v/v) formaldehyde and analyzed in a flow cytometer (BD Accuri C6, CellQuest v3.3 software, BD Biosciences).

Silica backpacks formation. hASCs were cultured in T-flasks, maintained under 5% CO_2 atmosphere at 37 °C and expanded until 80% of confluency or less before detachment using trypsin-EDTA (Thermo Fischer Scientific). The recovered cells were passed in a cell strainer of 40 µm to eliminate cell aggregates and then, seeded in petri dishes Ø60 mm, sterile, cell adherent (Sarstedt) with a low cell density of 125 000 cells/petri dish. 1 M of TEOS was hydrolyzed in 1 mM of aqueous HCl solution for 24 h. 1 M of APTES was hydrolyzed in 1 mM

of aqueous HCl solution at *RT* under magnetic stirring for 24 h. The solution with APTES was mixed with EtOH in a ratio of 1:1, and then used as followed. Briefly, after hASCs were adhered to the petri dishes, the medium of cells was discarded, and cells were washed with α-MEM without FBS and 1% P/S (FBS-free α-MEM). 1 mL of a solution of 0.4 mg mL^{-1} CHT-CAR dissolved in PBS was warmed in a water bath at 37 °C and then added to each petri dish. Afterwards the cells were left incubated for 10 min at 37.0 °C, 5% of CO_2. Later, CHT-CAR was discarded, and cells were washed with α-MEM w/0 FBS. 1 mL of solution FBS-free α-MEM: TEOS: APTES in the following proportion 950.0:12.5:37.5 was added and left incubate for 20 min at 37.0 °C, 5% of CO_2. Next, cells were washed 2 times with FBS-free α-MEM and then α-MEM was added. hASCs were then left to incubate at 37.0 °C, 5% of CO_2 until detachment and further used.

For some characterization assays APTES was diluted with other compounds with specific purposes: FITC was dissolved in 1 $mg.mL^{-1}$ of EtOH under magnetic stirring and protected from the light (flow cytometry, characterization, viability assay) and AB in 1 $mg.mL^{-1}$ of EtOH (Apoptosis/Necrosis assay, optical microscopy).

Flow cytometry analysis. Cells were stained with 5 µL of Vybrant™ DiD Cell-Labeling Solution (Invitrogen) was used for each million of cells suspended in 1 mL of DPBS and incubated at 37.5 °C for 20 min. The cells were washed 2 times with DPBS and resuspended in complete medium, followed by seeding in the petri dishes. The coating of cells was performed in darkness and FITC was used to stain the silica in the proportion described before. The cells were detached using 1 mL of Tryple Express and resuspended in 300 µL of DPBS. The flow cytometer was performed immediately. The resultant solution was passed in a cell strainer of 40 µm before measuring. The data was collected on BD Accuri C6 Plus flow cytometer and

post-acquisition analysis was performed with FlowJo software (Treestar, Ashland, OR, trial version).

Cell morphology analysis. hASCs were seeded in tissue culture coverslips, 13 mm with a cell density of $25x10^4$ cells. After, the partial coating was performed using AB, the cells were fixated in a solution of 2.5 % of glutaraldehyde diluted in 0.25 M in sodium cacodylate buffer for 6 h and dehydrated with a gradient of EtOH solutions (70, 80, 90 and 100 %) for 10 min each time. Then, the samples were let it dry at *RT*. Images were visualized by widefield fluorescence microscopy (Axio Imager M2, Carl Zeiss Microscopy, Germany). The acquired images were further analysed in Zeiss Zen Blue software (2017).

Scanning electron microscopy (SEM) and energy-dispersive X-ray spectroscopy (EDS). Cell aggregates from day 7 were previously fixed with a solution of 4% formaldehyde in PBS for 20 min followed by an ethanol gradient (60, 70, 80, 90, 95 and 100%) and then dried at *RT*. Before analysis, the samples were coated with a thin layer of evaporated carbon. Morphological and compositional images were acquired out by SEM (accelerating voltage 4 and 15 kV, SEM Hitachi, SU-70 instrument) coupled with an EDS (Bruker, Quantax 400 detector) with exposure time of 300 seconds.

F-actin filaments and Focal Adhesion Points Fluorescence Staining. Cells were fixed at RT in 4% formaldehyde in PBS for 20 min and permeabilized for 5 min with a solution of 0.1% Triton X-100. After washing with 3x with PBS, samples were stained with a vinculin polyclonal antibody conjugated with Alexa fluor 594 (Bioss Antibodies) diluted in 1:50 in PBS and left overnight at 4 ºC protected from the light. Afterwards, samples were stained with phalloidin – Flash Phalloidin Blue (Biolegend) in 1:40 in PBS for 45 min at *RT* followed by staining with

Helix NP® NIR (Biolegend) for 10 min at *RT*. Samples were visualized LSCM (LSM 880 Airyscan, Carl Zeiss Microscopy, Germany), and the acquired images were further analysed and processed in Zeiss Zen Blue software (2019).

Cell viability assays. Celltiter-Glo® 3D Cell viability assay (Promega, Madison, USA) was used to evaluate the viability of cells through ATP quantification coated and non-coated with silica in suspension for day 1. After the partial coatings cells with and without partial coatings were seeded in 24 ultra-low adhesion flat bottom well plates (Corning) with a density of 25 $x10^4$ cell per well. The assay was performed according to the manufacturer instructions. Briefly, CellTiter-Glo reagent was added at a 1:1 ratio, the samples were vigorously mixed for 5 min, and then incubated for 25 min at *RT*. Luminescence was recorded in a ultimodal microplate reader by using a white 96-well plate (Gen 5 software, Synergy HTX, BioTek Instruments, USA). A cell membrane viability assay was performed by using a fluorescence assay. Briefly, samples were collected and centrifuged at 300 g for 5 min and then stained with Calcein Blue AM (Invitrogen) and propidium iodide (PI) (Thermo Fischer Scientific) in PBS at 37 °C, 5% CO_2 for 20 min and protected from light. Afterwards, samples were visualized LSCM (LSM 880 Airyscan, Carl Zeiss Microscopy, Germany) and the acquired images were further processed in Zeiss Zen Blue software.

Apoptosis/Necrosis assay was performed to monitor apoptotic, necrotic and healthy cells with the apoptosis/necrosis detection Kit (Abcam) through LSCM (LSM 880 Airyscan, Carl Zeiss Microscopy, Germany). The assay was performed according to the manufacturer instructions. The resulting images were further analysed and processed in Zeiss Zen Blue software.

Total protein assay. Total protein quantification was performed using Micro BCA™ Protein Assay Kit. Cell samples were transferred to 1.5 mL centrifuge tubes. After centrifugation at

300 g for 5 min, the supernatant was discarded, and samples were washed with DPBS. Following a new centrifugation, samples were suspended in Triton X-100 0.5 % solution (500 µL per sample) for cell lysis. Then, samples were frozen at −80 °C at least overnight. Afterwards 2 cycles of freeze-thaw in an ultrasonic bath, at 37 ºC, 100 MHz were performed to destroy cell aggregates. Then, samples were defrosted, and the protein quantification was performed according to kit instructions. A standard curve for BSA analysis was generated with the provided BSA solution. After 2 hours of incubation at 37 ºC, absorbance was measured at 562 nm using a microplate reader with a clear 96-well bottom plate (Gen 5 software, Synergy HTX, Biotek Instruments, USA).

Total dsDNA Quantification. Total dsDNA quantification was performed using the assay kit Quant-iT PicoGreen (Life Technologies). Samples were transferred to 1.5 mL centrifuge tubes. After centrifugation at 300 g for 5 min, the supernatant was discarded, and samples were washed with PBS. Following new centrifugation, samples were suspended in Triton X-100 0.1% solution for cell lysis and left 1 hour, in a 37 °C water bath. Then, samples were frozen at −80 °C at least overnight. After 8 cycles of frosting and defrosting at ultrasonic bath, 37 ºC, 100 MHz to destroy cell aggregates, samples were defrosted and used according to the specifications of the kit. A standard curve for DNA analysis was generated with the provided dsDNA solution. After 10 min of incubation at *RT*, fluorescence was read at an excitation wavelength of 485/20 nm and 528/20 nm of emission using a microplate reader (Gen 5 software, Synergy HTX, Biotek Instruments, USA).

Cytoskeleton F-actin staining. Cells after 1 and 7 days of suspension were adhered to ibidi µ-slides 8 well. After adhesion, samples were fixed at *RT* in 4% formaldehyde in PBS, for 20 min, and permeabilized for 5 min, with a solution of 0.1% Triton X-100. After washing with 3x with

PBS, samples were stained with phalloidin – Flash Phalloidin FiTC (Biolegend) in 1:100 in PBS for 45 min at RT followed by staining with Hoechst 33342 (ThermoFischer) for 10 min at RT. Samples were visualized by widefield fluorescence microscopy (Axio Imager M2, Carl Zeiss Microscopy, Germany), acquired images were further analysed in Zeiss Zen Blue software (2017).

Injection assay: 700 000 cells per mL of partially coated and uncoated (control) cells were resuspended in a 2% w/v alginate solution dissolved in PBS pH=7.4 and filtered. Then, using a 1 mL syringe fitted with a 30 G needle and using a flow rate of 30 mL/h, cells were injected and incubated with Live/Dead solution for 30 min, 37ºC. The viability was then assessed through fluorescence microscopy and cells were counted using ImageJ software. The data was then analysed GraphPad Prism software (trial version). The assay was performed in triplicate.

Statistical analysis. Statistical differences were evaluated using one-way ANOVA test. A $p < 0.05$ was considered significant.

Supporting Information
Supporting Information is available from the Wiley Online Library or from the author.

Acknowledgements

The authors would like to acknowledge the financial support from the European Research Council (ERC) for project ATLAS (ERC2014-ADG-669858) and the Portuguese Foundation for Science and Technology (FCT) through the PhD grant PD/BD/139117/2018 (M. M. Maciel). This work was developed within the scope of the projects CICECO-Aveiro Institute of Materials (UIDB/50011/2020 & UIDP/50011/2020), COP2P (PTDC/QUI-QOR/30771/2017) and SUPRASORT (PTDC/QUI-OUT/30658/2017, CENTRO-01-0145-FEDER-030658) financed by national funds through FCT/MCTES and when appropriate co-financed by FEDER under the PT2020 Partnership Agreement and Programa Operacional Regional do Centro - Centro 2020, and within the scope of the Marine Biotechnology ERA-NET project BLUETEETH (ERA-MBT/0002/2015) financed by FCT under EU FP7 (Grant agreement number: 604814). Image acquisition was performed in the LiM facility of iBiMED, a node of PPBI (Portuguese Platform of BioImaging): POCI-01-0145-FEDER-022122. To Sónia G. Patrício for acquiring the SEM/EDS images.

Data available in article supplementary material

The data that supports the findings of this study are available in the supplementary material of this article.

Received: ((will be filled in by the editorial staff))
Revised: ((will be filled in by the editorial staff))
Published online: ((will be filled in by the editorial staff))

References

[1] V. M. Gaspar, P. Lavrador, J. Borges, M. B. Oliveira, J. F. Mano, *Adv Mater* **2020**, 32, e1903975.

[2] J. S. Liu, Z. J. Gartner, *Trends Cell Biol* **2012**, 22, 683.

[3] B. J. Kim, H. Cho, J. H. Park, J. F. Mano, I. S. Choi, *Adv Mater* **2018**, 30, e1706063.

[4] a) C. A. Custodio, J. F. Mano, *ChemNanoMat* **2016**, 2, 376; b) O. Hasturk, D. L. Kaplan, *Acta Biomater* **2019**, 95, 3; c) W. Youn, J. Y. Kim, J. Park, N. Kim, H. Choi, H. Cho, I. S. Choi, *Adv Mater* **2020**, 32, e1907001.

[5] X. Wang, H. C. Schroder, M. Wiens, U. Schlossmacher, W. E. Muller, *Adv Mar Biol* **2012**, 62, 231.

[6] a) I. Drachuk, M. K. Gupta, V. V. Tsukruk, *Advanced Functional Materials* **2013**, 23, 4437; b) A. M. Brokesh, A. K. Gaharwar, *ACS Appl Mater Interfaces* **2020**, 12, 5319.

[7] Á. J. Leite, M. B. Oliveira, S. G. Caridade, J. F. Mano, *Advanced Functional Materials* **2017**, 27.

[8] a) C. C. Perry, *Rev Mineral Geochem* **2003**, 54, 291; b) M. Sumper, E. Brunner, *Chembiochem* **2008**, 9, 1187; c) D. Medarevic, D. Losic, S. Ibric, *Hemijska industrija* **2016**, 70, 613.

[9] a) S. H. Yang, K. B. Lee, B. Kong, J. H. Kim, H. S. Kim, I. S. Choi, *Angew Chem Int Ed Engl* **2009**, 48, 9160; b) J. Lee, J. Choi, J. H. Park, M. H. Kim, D. Hong, H. Cho, S. H. Yang, I. S. Choi, *Angew Chem Int Ed Engl* **2014**, 53, 8056.

[10] K. A. Davis, P. J. Wu, C. F. Cahall, C. Li, A. Gottipati, B. J. Berron, *J Biol Eng* **2019**, 13, 5.

[11] Y. Teramura, H. Iwata, *Soft Matter* **2010**, 6.

[12] M. B. Oliveira, J. Hatami, J. F. Mano, *Chem Asian J* **2016**, 11, 1753.

[13] N. Nassif, J. Livage, *Chem Soc Rev* **2011**, 40, 849.

[14] D. Fischer, Y. Li, B. Ahlemeyer, J. Krieglstein, T. Kissel, *Biomaterials* **2003**, 24, 1121.

[15] S. Spirk, G. Findenig, A. Doliska, V. E. Reichel, N. L. Swanson, R. Kargl, V. Ribitsch, K. Stana-Kleinschek, *Carbohydr Polym* **2013**, 93, 285.

[16] J. L. Flanagan, P. A. Simmons, J. Vehige, M. D. Willcox, Q. Garrett, *Nutr Metab (Lond)* **2010**, 7, 30.

[17] a) W. Sajomsang, U. R. Ruktanonchai, P. Gonil, C. Warin, *Carbohydrate Polymers* **2010**, 82, 1143; b) N. Vallapa, O. Wiarachai, N. Thongchul, J. Pan, V. Tangpasuthadol, S. Kiatkamjornwong, V. P. Hoven, *Carbohydrate Polymers* **2011**, 83, 868.

[18] a) F. J. Pavinatto, L. Caseli, A. Pavinatto, D. S. dos Santos, Jr., T. M. Nobre, M. E. Zaniquelli, H. S. Silva, P. B. Miranda, O. N. de Oliveira, Jr., *Langmuir* **2007**, 23, 7666; b) F. J. Pavinatto, A. Pavinatto, L. Caseli, D. S. dos Santos, T. M. Nobre, M. E. D. Zaniquelli, O. N. Oliveira, *Biomacromolecules* **2007**, 8, 1633.

[19] a) G. M. Luz, J. F. Mano, *Nanotechnology* **2011**, 22, 494014; b) G. J. Owens, R. K. Singh, F. Foroutan, M. Alqaysi, C.-M. Han, C. Mahapatra, H.-W. Kim, J. C. Knowles, *Progress in Materials Science* **2016**, 77, 1.

[20] I. A. Rahman, M. Jafarzadeh, C. S. Sipaut, *Ceramics International* **2009**, 35, 1883.

[21] H. M. Lee, M. H. Kim, Y. I. Yoon, W. H. Park, *Mar Drugs* **2017**, 15.

[22] M. T. Stephan, D. J. Irvine, *Nano Today* **2011**, 6, 309.

[23] D. Raucher, M. P. Sheetz, *J Cell Biol* **2000**, 148, 127.

[24] Y. Ma, M. P. Neubauer, J. Thiele, A. Fery, W. T. S. Huck, *Biomater Sci* **2014**, 2, 1661.

[25] C. Huang, J. Dai, X. A. Zhang, *Biochim Biophys Acta* **2015**, 1850, 1261.

[26] F. Luan, L. Wei, J. Zhang, W. Tan, Y. Chen, F. Dong, Q. Li, Z. Guo, *Molecules* **2018**, 23.

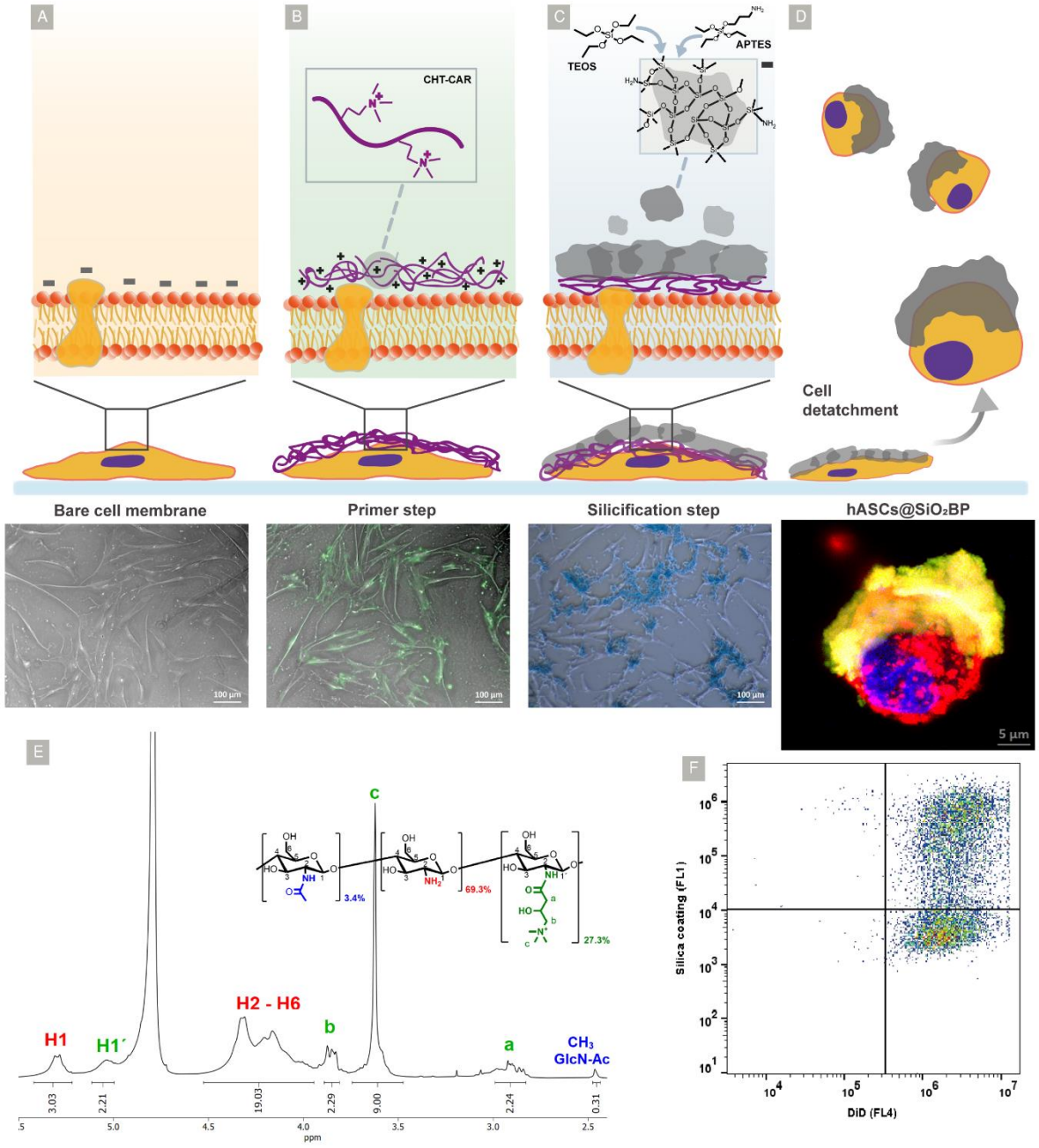

Figure 1. Scheme of silica backpack assembly in the surface of hASCs: A) The bare surface of cell membrane is negatively charged; B) In the primer step, CHT-CAR interacts with the cell membrane through electrostatic interactions forming a positively charged layer over the free surface of previously adhered cells. CHT-CAR modified with FITC (green) and adsorbed in the surface of cells via electrostatic interactions C) Afterwards, the silica solution is added, and condensation starts to occur forming the silica backpack. Morphological characterization of silica backpacks in hASCs: adherent cells bearing a silica partial coating (blue); D) Cells are detached from the cell surface with the partial coating forming the hASCs@SiO_2BP. Laser-scanning confocal microscopy (LSCM) of a partially coated single hASC in suspension conditions, individual channels – nucleus (Hoechst 33342, blue channel), cell membrane (wheat germ albumin – red channel) and silica (FITC, green channel) (Video S1); E) ^{1}H NMR spectra of CHT-CAR with characteristic peaks assigned and chemical structure; F) Flow cytometry dot

plot analysis of silicified hASCs populations. Around 57 % of cells are positive for DID (cell tracker) and FITC (silica marker) meaning cells with partial silica coatings.

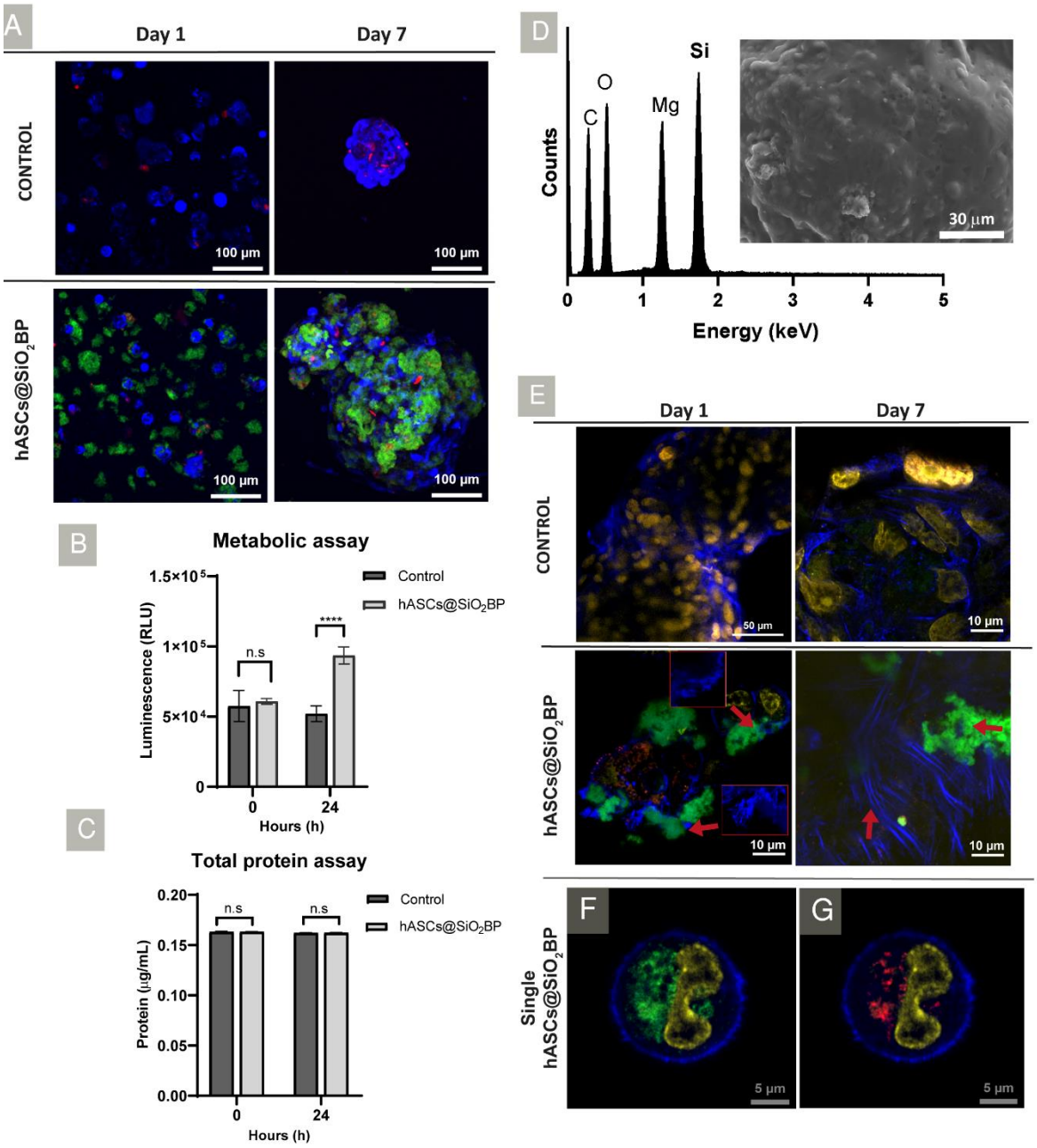

Figure 2. A) Cell viability assay at day 1 and 7: live cells (blue), dead cells (red) and silica (green); B and C) Metabolic activity and total protein quantification at 0 and 24 h. Data is presented as mean ± s.d., *n*=4; ****p < 0.0001, n.s, no statistical significance. D) SEM and EDS images of cell aggregates with silica backpacks from day 7, Si element is present confirming that even after 7 days, silica backpacks are part of cell aggregate. E) LSCM images of control and hASC@SiO_2BP both at day 1 and day 7. After one day in suspension, cells from control tend to aggregate faster compared to the other group. Red arrows indicate the longer F-actin filaments (blue) in both aggregates of hASC@SiO_2BP. At day 1, actin filaments prolonged where silica is present (green) and at day 7, hASC@SiO_2BP aggregates possess longer actin filaments compared to the controls; F) Single cell with focus on vinculin and G)

with silica. F-actin filaments (blue), nucleus (yellow pseudocolor), silica (green) and vinculin (red).

Silica partial coatings formed in the surface of human adipose stem cells are a novel and disruptive concept. The formation of these tough supports improved single cell survival and functionality in suspension environments. Also, these hybrid cells can be functionalized through silica with different molecules opening the possibility for various applications from sensing, drug delivery to microtissues formation.

Marta M. Maciel, Tiago R. Correia*, Vítor M. Gaspar, João M. M. Rodrigues, Insung S. Choi, João F. Mano*

Partial coated stem cells with bioinspired silica as new generation of cellular hybrids materials